

Enhancement of kinetic energy fluctuations due to expansion

A. Chernomoretz,^{1,*} F. Gulminelli,^{2,†} M.J. Ison,¹ and C.O. Dorso¹

¹ Departamento de Física, Universidad de Buenos Aires,
Buenos Aires, Argentina.

²LPC Caen (IN2P3-CNRS/Ensicaen et Université) F-14050 Caen Cédex. France

(Dated: November 5, 2018)

Global equilibrium fragmentation inside a freeze out constraining volume is a working hypothesis widely used in nuclear fragmentation statistical models. In the framework of classical Lennard Jones molecular dynamics, we study how the relaxation of the fixed volume constraint affects the posterior evolution of microscopic correlations, and how a non-confined fragmentation scenario is established. A study of the dynamical evolution of the relative kinetic energy fluctuations was also performed. We found that asymptotic measurements of such observable can be related to the number of decaying channels available to the system at fragmentation time.

PACS numbers: 25.70 -z, 25.70.Mn, 25.70.Pq, 02.70.Ns

I. INTRODUCTION

The multifragmentation phenomenon has attracted the attention of the intermediate/high energy nuclear community since more than a decade. Starting in the 1980's, a lot of attention has been paid to the identification and characterization of the occurrence of a nuclear liquid-gas phase transition. On one hand, indications of critical behavior were obtained assuming a Fisher-like scaling relation for fragment mass distributions [1, 2, 3, 4]. On the other, it has been claimed that the observed critical behavior in static observables is compatible with a first order phase transition [5, 6, 7, 8, 9].

As in nuclear fragmentation experiments one only has access to asymptotic observables, the fragmentation stage of the dynamic evolution must be reconstructed using simplified models. To accomplish this task, the most widely used statistical models of the MMMS [10] or SMM [11] type, replace the intractable problem of quantum N-body correlations with a non interacting gas of fragments confined with sharp boundary conditions [10, 11]. A distinctive feature of these equilibrium fragmentation models is that a vapor-branch can be recognized in the system caloric curve (CC). Moreover, in the statistical sampling of configurations, the observed asymptotic flux is exclusively associated with the mean Coulomb energy of partitions inside the constraining volume. Collective motions are completely disregarded before and during the fragment formation stage.

On the contrary, when fragmentation is considered in a non-constrained free-to-expand scenario qualitatively different features are found. In this case a local equilibrium picture replaces the global one, and a characteristic flattening of the caloric curve at high energy can be found [12]. This happens as a direct consequence of the presence of a collective degree of freedom: the expansive

motion behaves like a heat sink, and precludes the disordered kinetic energy associated with the system temperature to increase without bounds [13]. These last remarks rise some reasonable concerns regarding the sharp constraining volume working hypothesis that are worth to be analyzed.

In recent contributions the study of the behavior of the relative kinetic energy fluctuations, $A_K \equiv N\sigma_K^2 / \langle K \rangle^2$, has received considerable attention. It has been shown [7, 14] that partial energy fluctuations can be used to measure the EOS, and to extract information of the possible phase transition occurring in finite systems like multifragmenting nuclei. Negative specific heats are expected to signal first order phase transitions in these systems [9, 15]. Taking into consideration that kinetic energy fluctuations and the system's specific heat are related by [16]:

$$\frac{1}{N} \langle \sigma_K^2 \rangle_E = \frac{3}{2\beta^2} \left(1 - \frac{3}{2C}\right) \quad (1)$$

(where $\beta = 1/kT$) negative values of the specific heat are expected to appear whenever σ_K^2 gets larger than the corresponding canonical expectation value: $\frac{3N}{2\beta^2}$.

Using a classical molecular dynamics model it has been already shown in [17] that large relative kinetic fluctuations do take place in confined classical isolated systems, provided that the constraining volumes are large enough to accommodate non-overlapping configurational fragments. In this paper we want to pursue with the system's characterization by studying its temporal evolution once we remove the constraining walls within which it was equilibrated. Our aim is to understand how much memory of the initial configuration is kept in the asymptotic fragmentation patterns which are accessible experimentally. To that end we will focus on the dynamical evolution of fragment mass distribution functions (MDF), and the relative kinetic energy fluctuation, A_K , that turns out to be a useful tool to probe the unconstrained fragmentation scenario.

*Electronic address: ariel@df.uba.ar

†Member of the Institut Universitaire de France.

II. THE MODEL

The system under study is composed by excited drops made up of 147 particles interacting via a 6-12 Lennard Jones potential with a cut-off radius $r_c = 3\sigma$. Energies are measured in units of the potential well (ϵ), σ characterizes the radius of a particle and m is its mass. We adopt adimensional units for energy, length and time such that $\epsilon = \sigma = 1$, $t_0 = \sqrt{\sigma^2 m / 48\epsilon}$. Our particles are uncharged and the inclusion of Coulomb is certainly a necessary step to insure that our results are pertinent to the nuclear fragmentation problem [18]. However, the fact that the nuclear force and the van der Waals interaction both share the same general features (i.e. short range repulsion plus a longer range attraction) supports the use of this simplified classical model to obtain qualitatively meaningful results in the nuclear case, and serves also to explore phenomena of greater generality. The initial condition is chosen as a spherical confining ‘wall’, introducing an external potential $V_{wall} \sim (r - r_{wall})^{-12}$ with a cut off distance $r_{cut} = 1\sigma$. The set of classical equations of motion were integrated using the well known velocity Verlet algorithm, which preserves volume in phase space[19].

Using this system, we have performed the following molecular dynamics (MD) experiments. First, we let the system equilibrate inside the constraining volume at a chosen density. We call this initial condition the *constrained state*. Afterwards, we remove the constraining walls, and let the system evolve for a very long time, such that the fragment composition reaches stability. This will be referred to as the *asymptotic stage*.

One of the key observables to study phase transformations from a morphological point of view is the fragment mass distribution. The simplest and more intuitive cluster definition is based on correlations in configuration space: a particle i belongs to a cluster C if there is another particle j that belongs to C and $|\mathbf{r}_i - \mathbf{r}_j| \leq r_{cl}$, where r_{cl} is a parameter called the clusterization radius. In this work we took $r_{cl} = r_{cut} = 3\sigma$. The algorithm that recognizes these clusters is known as the “Minimum Spanning Tree” (MST). The main drawback of this method is that only correlations in \mathbf{r} -space are used. MST clusters give no meaningful information about the fragmentation dynamics when the system is dense.

A more robust algorithm is based on the analysis of the so called “Most Bound Partition” (MBP) of the system, introduced in Ref. [20]. The MBP is the set of clusters $\{C_i\}$ for which the sum of the fragment internal energies attains its minimum value:

$$\begin{aligned} \{C_i\} &= \operatorname{argmin}_{\{C_i\}} \left[E_{\{C_i\}} = \sum_i E_{int}^{C_i} \right] \\ E_{int}^{C_i} &= \sum_{j \in C_i} K_j^{cm} + \sum_{j,k \in C_i, j \leq k} V_{jk} \end{aligned} \quad (2)$$

where the first sum in (2) is over the clusters of the partition, K_j^{cm} is the kinetic energy of particle j measured

in the center of mass frame of the cluster which contains particle j , and V_{ij} stands for the inter-particle potential. It can be shown that clusters belonging to the MBP are related to the most-bound density fluctuation in $\mathbf{r}\text{-}\mathbf{p}$ space [20]. The algorithm that finds the MBP is known as the “Early Cluster Recognition Algorithm” (ECRA).

In a previous contribution we studied the EOS of a finite, constrained, and classical system using cluster distributions properties in phase space and in configurational space [17]. Figure 1 summarizes our findings. In the upper panel we show the density dependence of the system energy E_{crit} at which transition signals (power-law mass spectrum, maxima in the second moment of the mass distribution, and normalized mean variance) are detected. Given a confined system with a density value ρ , for $E < E_{crit}(\rho)$ a big ECRA cluster can be found, whereas for $E > E_{crit}(\rho)$ a regime with high multiplicity of light ECRA clusters dominates. The lower panel shows the same transition line in the most usual (T, ρ) plane (see [17] for details).

According to the calculated critical exponents τ , and γ , three density regions could be identified. One (very low density limit, region labeled A in Figure 1) in which the boundary conditions are almost ineffective, and a back-bending of the caloric curve can consequently be observed even in the isochore ensemble [21]. Another one (region C in Figure 1), corresponding to the high density regime, in which fragments in phase space display critical behavior of 3D-Ising universality class type. And an intermediate density region (region B in Figure 1), in which power-laws are displayed but can not be associated to the above mentioned universality class (see Ref. [17]). The thermodynamic critical point of the liquid-gas phase transition ($\rho_c \approx 0.35\sigma^{-3}$, $T_c \approx 1.12\epsilon_0$) corresponds to the meeting point of these two last regions.

Having these results in mind, we chose the following density values, $\rho_1 = 0.026\sigma^{-3}$, $\rho_2 = 0.10\sigma^{-3}$, $\rho_3 = 0.6\sigma^{-3}$ (i.e. one from each relevant region of the EOS) in order to study the effect of the dynamic evolution on the observables that characterize the initially equilibrated confined systems.

III. TIME EVOLUTION OF PARTICLE CORRELATIONS

In order to explore the effects of constrain removal on the fragment spectra of the systems under study, we compare the confined ECRA-fragment mass distribution of the constrained system, against the corresponding MST asymptotic ones.

In Figure 2 we show MDF calculations performed over systems initially constrained at the density values above mentioned (from left to right: ρ_1, ρ_2 , and ρ_3) with different total energies (increasing E from bottom to top). For a given set of values (E, ρ) the confined state ECRA-fragment mass spectra and the corresponding asymptotic

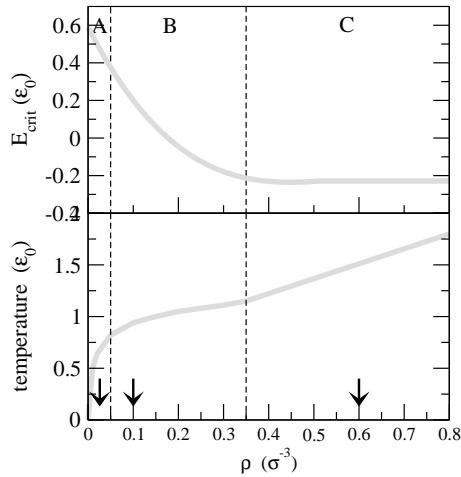


FIG. 1: Upper panel: energy E_{crit} at which transition signals are detected in a confined, finite size fragmenting system, as a function of the system density. Lower panel: same transition line in the temperature-density plane (see text for details). The arrows indicate the density values considered for the present calculations.

MST-fragment mass spectra can be compared. It should be kept in mind that for ρ_2 and ρ_3 initial states present just one big fragment according to the MST algorithm.

For the case of an initially extremely diluted system (first column in Figure 2) confined states are already fragmented in configurational space. The corresponding asymptotic fragment structure remains essentially unaltered, aside of the evaporation of light clusters from the heaviest fragment.

On the other hand, it can be seen that for initial higher densities (ρ_2 , and ρ_3) the $\mathbf{q}-\mathbf{p}$ correlations of the confined state, probed by ECRA partitions, are modified by the dynamics that follows the walls removal. For these densities, the size of the biggest clusters detected in both, the confined and asymptotic stages, seem to agree to a high degree. However noticeable differences are found in relative abundances, specially for intermediate size fragments (IMF).

The development of an expansive flux modifies the correlation pattern observed in phase space for initially dense confined configurations acting as a memory loosing mechanism of their initial fragment structure. This result implies that even a subcritical density relatively diluted as the $\rho = 0.1\sigma^{-3}$ case cannot be taken as a freeze out configuration, since freeze out by definition implies a persistency of the information up to asymptotic times. It is then clear that between confined states and corresponding asymptotic configurations, the intermediate stage, characterized by the development of expansive collective motion and the consequent expansion of the system, plays a crucial role in the process of fragment formation. The relative similarity between the asymptotic distributions originated from the $\rho = 0.1\sigma^{-3}$ and $\rho = 0.6\sigma^{-3}$ initial conditions, suggests that the

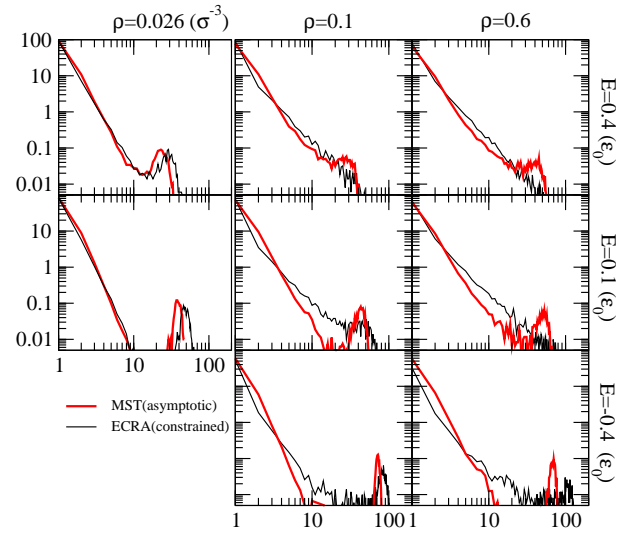


FIG. 2: Confined ECRA vs asymptotic MST mass spectra calculated for 3 different initial densities: $\rho = 0.026\sigma^{-3}$, $0.1\sigma^{-3}$, and $0.6\sigma^{-3}$ shown in first, second, and third columns respectively.

expansion dynamics leads to a fragmentation pattern essentially determined by the total energy. On the other hand the distribution originated from the initially most diluted system is sensibly different from the denser cases. Indeed the size of the heaviest fragment is smaller and the IMF distribution is steeper in this case. This means that a fragmentation pattern originated from an expansion process is not equivalent to an equilibrated freeze out with sharp boundary conditions. It has been proposed[22] that such a fragmentation pattern may still be described in statistical terms through information theory with the constraints of a fluctuating volume and a radial flow. The possible pertinence of such a scenario is left to future investigations.

IV. KINETIC ENERGY FLUCTUATIONS

As was stated in the introduction, fragmenting finite systems at microcanonical equilibrium display negative specific heats whenever relative kinetic energy fluctuations surpass the canonical expected value. This is theoretically expected in the liquid-gas phase transition of small systems if the volume is not constrained by sharp boundary conditions[23]. Consistently it has been suggested that the magnitude A_K can be used to identify the occurrence of first order phase transitions in such systems [7]. If the equiprobability of the different configuration microstates is assumed, as it is by construction the case in our initial conditions, $K = K(T)$, and

$$A_K \equiv N \frac{\sigma_K^2}{\langle K \rangle^2} \propto \frac{\sigma_K^2}{T} \quad (3)$$

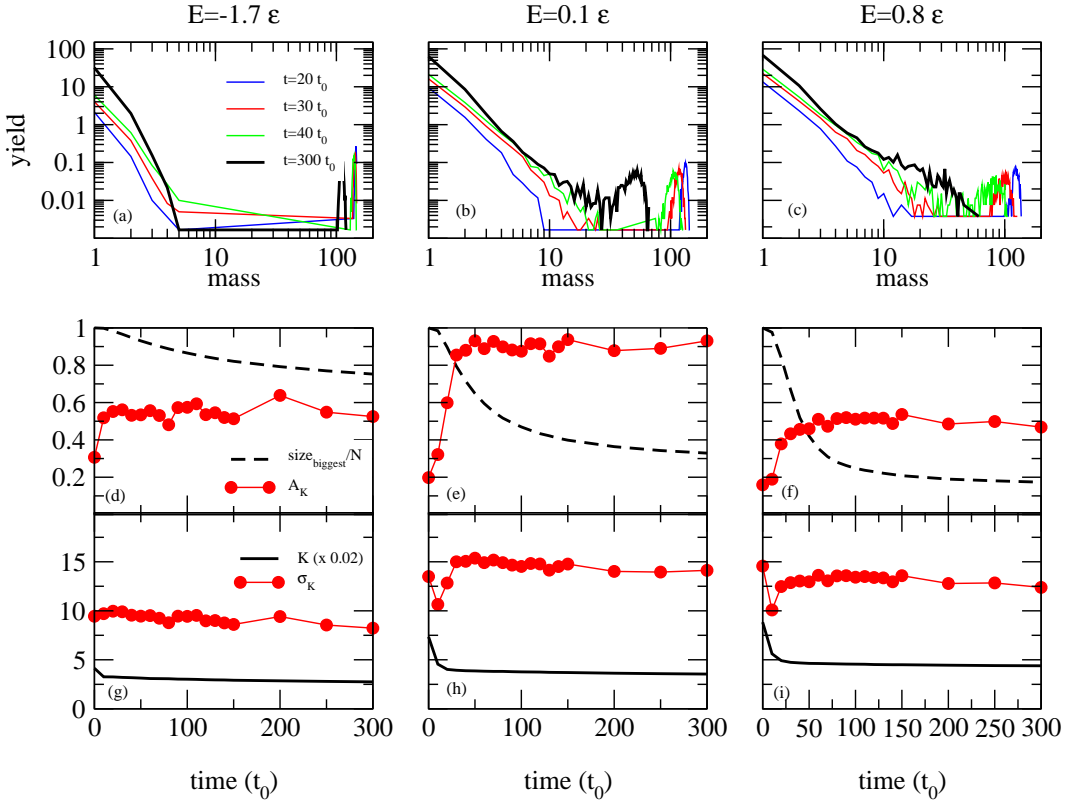


FIG. 3: Upper panels (3.a, 3.b, 3.c): MST fragment spectra calculated at $t = 20, 30, 40$ and, $300t_0$ for a $\rho = 0.6\sigma^{-3}$ system at three different energies. Middle panels (3.d, 3.e, 3.f): $A_K(t)$ (red circles) and MST-biggest cluster mass (dashed lines) as a function of time. Lower panels (3.g, 3.h, 3.i): Total kinetic energy (solid line) and Kinetic energy fluctuations (red circles) as a function of time.

In this way, the system specific heat can be calculated through Eq. 1 knowing both, $\langle K \rangle$, and σ_K^2 .

Since the dynamics of the expansion tends to drive the system into a rather rarefied state, and allows event by event volume fluctuations which are suppressed by the sharp boundary, it is interesting to see whether such abnormal fluctuations can be reached in a fully dynamical simulation. In this case the average kinetic energy cannot be associated to a temperature any more, and the relationship expressed in Eq. 1 can no longer be invoked to estimate the system specific heat. However meaningful information can still be obtained from A_K when we resort to dynamical quantities only. In Figure 3 we show the time evolution of MST mass spectra (panels 3.a, 3.b, and 3.c), A_K (panels 3.d, 3.e, and 3.f), K , and σ_K (panels 3.g, 3.h, and 3.i) calculated for a system initially confined at a density $\rho = \rho_3 = 0.6\sigma^{-3}$, for three different energies. We also show in panels 3.d, 3.e, and 3.f, the corresponding time evolution of the normalized mass of the biggest MST fragment (dashed line).

From this figure we can see that the time at which A_K attains its asymptotic value (panels d, e, and f) signals the time at which, in average, the fragmentation pattern is settled for each event of a given energy and initial density values. To support this idea, in the upper

panel of Figure 3 we show MST spectra calculated at different times. It can be noticed that at $t \sim 40t_0$ a significative proportion of the mid-size asymptotic MST-fragments are already produced, i.e. internal surfaces already appeared. For later times the big residue evolves just by light particles evaporation.

As a result of the expansion, physical observables like A_K change in time during a relatively short lapse after which they attain almost constant values. A *freeze-out* time, τ_{fo} , can then be introduced, after of which the evolution becomes almost irrelevant. Moreover, Figures 3.d, 3.e, and 3.f also indicate that asymptotic measurements allow to reconstruct quantities as early as $\tau_{fo} \sim 40t_0$.

This observation agrees with previous results. In reference [24] it was shown that for unconstrained systems a time of fragment formation (τ_{ff}), related to the stabilization of microscopic clusters composition, can be defined. For the cases studied we found that $\tau_{ff} \sim \tau_{fo}$, meaning that the information is frozen once the fragment surfaces have developed. From the lower panels we see that the variance of the kinetic energy, σ_K , also attains its asymptotic value at this time. It is important to stress that this definition of a freeze out time corresponds to a MaxEnt principle within the constraints imposed by the dynamical

cal evolution. As such, this definition does not imply that the freeze out configuration corresponds to an absolute entropy maximum, i.e. to a thermodynamic equilibrium.

For the lowest considered energy, σ_K does not change significantly in time and this stays true if we change the initial density. This is the expected behavior as the system, in almost every realization, only evaporates light clusters in its early evolution, and a big fragment is always present almost independent of the system volume. On the other hand, for the more energetic cases the initial decrease of σ_K can be related to the preequilibrium dynamics that involves a flux development (expansion) and prompt emission of light particles. Afterwards, the development of internal surfaces gives rise to a large set of possible decaying channels (opening of phase space) that is responsible for the σ_K enhancement.

A_K asymptotic values characterize the number of different fragmentation configurations compatible with the total energy constraint. Large kinetic energy fluctuations reflect large potential energy fluctuations that can be directly related to event by event final cluster distributions. In this sense K fluctuations can be associated with the available number of decaying channels for a given energy, i.e. with the microcanonical entropy.

V. DISCUSSION

We summarize in Fig.4 the results of A_K calculations obtained so far. In the upper panel we show the fluctuations in kinetic energy for the three confined states analyzed at densities ρ_1 (circles), ρ_2 (squares), and ρ_3 (diamonds). The solid lines are not a fit, but an A_K estimation using information from the respective system's caloric curve. The nice agreement between the lines and the symbols demonstrates the quality of our numerical sampling. In the middle and lower panels we report the same quantity calculated at the time of σ_K stabilization (as was mentioned above, this time is well-correlated with the time of fragment formation) and for the corresponding asymptotic configurations respectively. In the upper panel the horizontal dotted-dashed line depicts the expected canonical value for A_K . We included it also in the middle and bottom panels, only as a reference value. In the fluctuation analysis performed on experimental heavy ion data, the average kinetic energy is approximately corrected for evaporation and for the Coulomb boost, while fluctuations are assumed to be correctly given by the asymptotic measurement [9]. This means that the middle panel is the most relevant for a comparison with experimental data.

The confined state with density ρ_1 , that belongs to region A in the phase diagram of Fig.1 (full circles) displays a maximum that is well above the canonical value. As such there is a region for which the thermal response function is negative. On the other hand for the confined states ρ_2 and ρ_3 , that belong to region B and C respectively of the phase diagram, the corresponding values

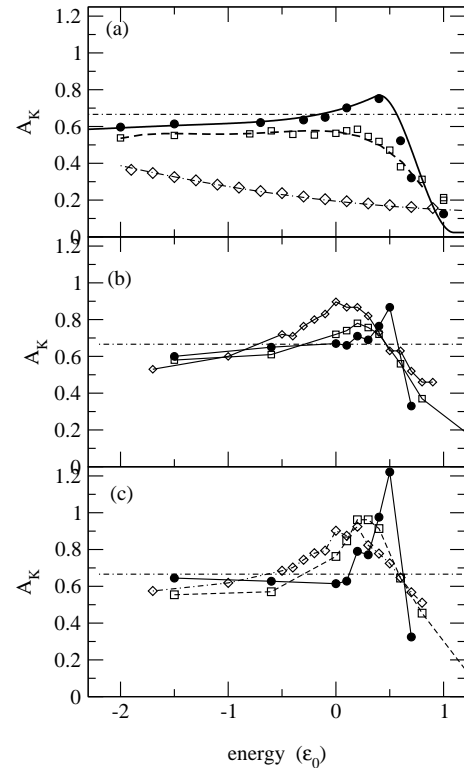


FIG. 4: Top: Relative kinetic energy fluctuations as a function of the total energy for densities ρ_1 (circles), ρ_2 (squares), and ρ_3 (diamonds). Middle: same as top, but evaluated at the time of σ_K stabilization ($t(\rho_1) \sim 5t_0$, $t(\rho_2) \sim 30t_0$, $t(\rho_3) \sim 40t_0$). Bottom: same as top, but evaluated for asymptotic configurations. See text for details.

of the kinetic energy fluctuations are always below the canonical value.

If we now turn our attention to the results of the same calculation but now performed on the states resulting from removing the confining walls and allowing the system to expand and fragment, the results displayed in the middle and lower panel of Fig.4 are obtained. Almost independent of the initial condition, the normalized fluctuations fall on a curve which is mainly determined by the total energy and fairly close to the thermal response of an initially diluted system in microcanonical equilibrium. The kinetic energy fluctuations that were below the threshold for all energies have been clearly enhanced in the energy region defined by $0 \leq E \leq 0.5\epsilon_0$. This feature, as was already mentioned, reflects the existence of quite different available decaying channels that are explored by the systems dynamics. In particular, at these energies, partitions with big residues on one hand, and high multiplicity partitions with no such big structures on the other, can be produced giving rise to power-law like distributions. If we look at the asymptotic stage (lower panel), the picture is somewhat blurred by secondary evaporation that continuously decreases the av-

verage kinetic energy without affecting the fluctuation. It is worth noticing that at time of fragment formation the average system volume is approximately independent of the initial density: this means that for all initial conditions the information is frozen when the system reaches the region of the phase diagram (region A of figure 1) where abnormal fluctuations are expected in equilibrium, i.e. in the case of a full opening of the accessible phase space. This observation may suggest that the collective motion leads the system to a low density freeze out configuration which is not far away from a thermodynamic equilibrium. However, to make any conclusion about the possible degree of equilibration and the characteristics of the relevant statistical ensemble, a more detailed analysis is needed.

VI. CONCLUSION

In conclusion, in this work we have shown that for free to expand fragmenting systems, initially equilibrated within sharp boundary conditions, an intermediate stage exists where new microscopic correlations arise. This happens in the presence of a collective expansive motion that induce internal surfaces to appear in the system, preceding the formation of well defined asymptotic clus-

ters.

In addition, the analysis of the dynamical evolution of A_K turned out to be fruitful. On one hand it allowed us to give a physically meaningful estimation of the freeze-out time, which turned out to be in good agreement with the corresponding fragment formation time. On the other, it was shown that a link can be established between asymptotic values of that observable and mass distribution functions. In isolated systems, like the one studied here, a maximum of A_K as a function of the system energy can be related to a noticeably enlargement of the number of possible decaying channels. This enhancement of the relative kinetic energy fluctuation can thus be associated with an opening of phase space that is expected in phase transitions taking place in finite isolated systems.

It is worth noting that even if the non-constrained fragment formation stage seems to provide a quite effective memory loosing mechanism (see Fig. 2), preliminary results support the idea that information on the initial system density can still be retrieved from certain asymptotic cluster configurational features. This analysis, along with a thorough characterization of the system equilibration properties at τ_{fo} is currently under progress.

This work was done with partial financial supports from UBA and CONICET.

[1] A. S. Hirsh *et al.* *Phys. Rev. C*, vol. 29, p. 508, 1984.
[2] J. B. Elliott *et al.* *Phys. Rev. Lett.*, vol. 85, p. 1194, 2000.
[3] X. Campi *Phys. Lett. B*, vol. 208, p. 351, 1988.
[4] A. Bonasera, M. Bruno, C. O. Dorso, and P. F. Mastinu *Nuovo Cimento*, vol. 23, p. 2, 2000.
[5] F. Gulminelli and P. Chomaz *Phys. Rev. Lett.*, vol. 82, p. 1402, 1999.
[6] S. D. G. J. Pan and M. Grant *Phys. Rev. Lett.*, vol. 80, p. 1181, 1998.
[7] P. Chomaz and F. Gulminelli *Nucl. Phys. A*, vol. 647, p. 153, 1999.
[8] F. Gulminelli, P. Chomaz, and V. Duflot *Europhys. Lett.*, vol. 50, p. 434, 2000.
[9] M. D'Agostino *et al.* *Phys. Lett. B*, vol. 473, p. 219, 2000.
[10] D. H. Gross *Rep. Prog. Phys.*, vol. 53, p. 605, 1990.
[11] J. B. Bondorf *et al.* *Phys. Report.*, vol. 257, p. 133, 1995.
[12] A. Chernomoretz, M. Ison, S. Ortiz, and C. Dorso *Phys. Rev. C*, vol. 64, p. 24606, 2001.
[13] A. Strachan and C. O. Dorso *Phys. Rev. C*, vol. 55, p. 775, 1997.
[14] P. Chomaz, V. Duflot, and F. Gulminelli *Phys. Rev. Lett.*, vol. 85, p. 3587, 2000.
[15] D. H. Gross, *Microcanonical Thermodynamics*. Singapore: World Scientific, 2001. Lecture notes on Physics 66.
[16] J. L. Lebowitz, J. K. Percus, and L. Verlet *Phys. Rev.*, vol. 153, p. 250, 1967.
[17] A. Chernomoretz, P. Balenzuela, and C. Dorso *Nucl. Phys. A*, vol. 723, p. 229, 2003.
[18] M. Ison and C. O. Dorso *Physical Review C*, 2004. In press.
[19] D. Frenkel and B. Smit, *Understanding Molecular Simulation, from Algorithms to Applications*. San Diego Academic Press, 1996.
[20] C. O. Dorso and J. Randrup *Phys. Lett. B*, vol. 301, p. 328, 1993.
[21] F. Gulminelli *et al.* *Phys. Rev. E*, vol. 68, p. 026120, 2003.
[22] F. Gulminelli and P. Chomaz *Nucl. Phys. A*. in press.
[23] P. Chomaz *et al.*, “Dynamics and thermodynamics of systems with long range interactions,” in *Lecture Notes in Physics vol 602*, Springer, 2002.
[24] A. Strachan and C. O. Dorso *Phys. Rev. C*, vol. 59, p. 285, 1999.